J. Fluid Mech. (1969), *vol.* 39, *part* 2, *pp.* 227–255
Printed in Great Britain

On the interaction of an infinite shallow draft cylinder oscillating at the free surface with a train of oblique waves

By C. J. GARRISON†
University of Washington, Seattle, Washington

(Received 7 January 1969 and in revised form 21 April 1969)

This paper presents the practical and rigorous solution of the potential flow problem associated with the oscillation of a shallow-draft cylinder of infinite length on a free surface. The problem is three-dimensional to the extent that the amplitude of the cylinder oscillation is periodic along its axis as well as with time. The complementary problem associated with the interaction of the fixed cylinder with an incident wave train aligned at some oblique angle with respect to the cylinder axis is also treated. The use of a Green's function reduces the problem to an integral equation which is solved numerically. Numerical results are computed for pressure amplitude distributions, force coefficients, added mass and damping coefficients, transmission and reflexion coefficients and wave height ratios.

Introduction

In the design of such structures as floating breakwaters and floating bridges, dynamic forces due to structure/wave interaction are important factors. Not only the forces exerted on the structure due to wave action but the hydrodynamic forces associated with the elastic response of the structure are important. The motion of a given structure depends on its elastic properties, its mass distribution, and its wetted shape as well as the wave system exciting its motion. This paper deals with the hydrodynamic aspects of such a wave/structure interaction problem without attempting to determine the motion of a specific structure. The geometry under consideration is an infinite length, shallow-draft cylinder located at the free surface.

In dealing with the motion of a structure in the presence of wave action it is usual to consider the hydrodynamic aspects of the problem in two parts: (i) forces acting on the structure due to the incident wave, assuming the structure to be fixed; (ii) the added mass and damping forces acting on the structure, assuming the structure to be oscillating in otherwise still water. The complete problem of the structure excited by wave action with resulting oscillations can be represented by the superposition of the two types of fluid motion.

The boundary-value problem arising from the motion of a floating body of arbitrary shape has been formulated by John (1950) but, except for certain simple shapes, the resulting equations are difficult and have not been numerically

† Present address: Dept. of Civil Engineering, Texas A & M University.

evaluated. Ursell (1949) developed a procedure for treating the two-dimensional case of a circular cylinder oscillating in still water. His method may be extended to elliptic cross-sections and other rather general two-dimensional forms and some results of this extension have been published by Porter (1960). Yu & Ursell (1961) treated the problem of a semi-submerged circular cylinder oscillating vertically in finite depth water and Gidlund (1963), using the same basic method, treated the complementary problem of wave interaction with a fixed circular cylinder semi-submerged in water of finite depth. Using the Green's function approach, Kim (1965) treated the case of an elliptical cylinder and ellipsoid oscillating on the free surface. MacCamy (1961, 1964) treated the two-dimensional motion associated with a shallow-draft cylinder oscillating in heave and roll in still water. MacCamy formulated the problem as a regular perturbation problem for small values of the draft-beam ratio and calculated the first-order solution for an elliptical shape.

Much less work has been done on the wave/structure interaction problem involving waves with crests not parallel to the cylinder axis. MacCamy (1957) formulated the boundary-value problem arising from the interaction of waves with an infinite strip (zero-draft cylinder) located at the free surface, the waves being incident with crests oriented at some oblique angle with respect to the axis of the strip. Neither a numerical procedure nor numerical results were, however, obtained. Levine (1965) addressed himself to a similar problem involving wave interaction with a completely submerged circular cylinder near the free surface wherein, again, the waves were oriented at some oblique angle with respect to the cylinder axis. Transmission and reflexion coefficients only were calculated for this case.

The present paper deals with the interaction of a train of regular deep water waves with a shallow-draft cylinder floating at the free surface, as well as the complementary problem associated with the fluid motion induced by the oscillation of the cross-section of the cylinder in each of its three degrees of freedom (heave, roll and sway). The amplitude of each of the modes of oscillations is assumed to vary sinusoidally along the length of the cylinder. The problem is formulated as a boundary-value problem in the parameter, ϵ = draft/beam ratio, and the zeroth-order solution (corresponding to zero-draft cylinder or a plate at the free surface) is considered in detail. The zero-draft problem is formulated in terms of the source function, or Green's function, which results in an integral equation of the second kind, of a form similar to that used by MacCamy (1957). This resulting integral equation is solved by numerical methods by use of a digital computer and numerical results are presented for pressure amplitude distributions, transmission and reflexion coefficients, wave force and added mass and damping coefficients and wave height ratios.

These hydrodynamic quantities are functions of the frequency, σ, or wavelength, $\bar{L}$, and the angle the wave crests make with the longitudinal axis of the cylinder, β, or, more precisely, functions of $a = \bar{a}\sigma^2/g = 2\pi\bar{a}/\bar{L}$ and $\nu = a\sin\beta, g$ being the acceleration of gravity and $\bar{a}$ the cylinder half-beam. Numerical results are presented for a zero-draft cylinder and, in order to gain some confidence in these results, comparisons are made with previous results of others,

with asymptotic solutions and by use of Haskind's relations. All of these comparisons were successful and, therefore, it would seem, on the basis of the limited evidence available, that the present method yields accurate results.

There is a fundamental limitation to the present numerical method, however. The kernel of the integral equation oscillates rapidly as a increases. Thus, unless the subdivisions are kept small the quadratures occurring in the present numerical method become inaccurate. We note, however, that the normal waves are the most critical with respect to this limitation since the fluctuation wavelength increases with ν/a. The numerical results in this paper extend to values of a of approximately six, which covers the range of practical interest.

Formulation of the problem

The problem set forth herein deals with the fluid motion induced by the oscillations of a long, shallow-draft cylinder on the free surface as well as the fluid motion associated with the interaction of the fixed cylinder with a train of regular waves incident at some oblique angle with respect to the axis of the cylinder. Essentially four separate problems are dealt with: (i) the scattering of waves incident at some oblique angle due to the presence of a fixed cylinder; (ii) the fluid motion produced by the shallow-draft cylinder oscillating in heave, roll and sway, one at a time, the amplitude of the motion varying sinusoidally along the length of the cylinder.

Consider the region lying outside the infinite cylinder (extending from $\bar{z} = -\infty$ to $+\infty$) and below the free surface to be filled with an incompressible, inviscid liquid (see figure 1). Assuming that the motion started from rest a velocity potential, Φ, can be defined by

$$\overline{V} = \nabla\Phi(\bar{x}, \bar{y}, \bar{z}, t), \tag{1}$$

where $\overline{V}$ is the fluid velocity vector and where Φ must satisfy the Laplace equation,

$$\nabla^2\Phi(\bar{x}, \bar{y}, \bar{z}, t) = 0 \tag{2}$$

within the fluid region.

The amplitude of the motion will be considered small in comparison to other lengths involved and, consequently, the square of the fluid velocity occurring in Bernoulli's equation can be neglected, yielding the wave height in terms of the time derivative of the velocity potential as

$$\bar{\eta}(\bar{x}, \bar{z}, t) = (1/g)\,\Phi_t(\bar{x}, 0, \bar{z}, t), \tag{3}$$

when the wave height is considered small. The usual linearized free surface boundary condition,

$$\Phi_{\bar{y}}(\bar{x}, 0, \bar{z}, t) + (1/g)\,\Phi_{tt}(\bar{x}, 0, \bar{z}, t) = 0, \tag{4}$$

for all values of $\bar{x}$ outside the cylinder, follows from (3).

The velocity potential for a progressive deep water wave system (incident wave) approaching the cylinder with crests aligned at some angle, β, with respect to the $\bar{z}$ axis of the cylinder is given by

$$\Phi_w(\bar{x}, \bar{y}, \bar{z}, t) = \mathrm{Re}\left[-i\frac{g}{\sigma}\bar{\eta}_w^0\, e^{[K\bar{y} + i(K\bar{x}\cos\beta + K\bar{z}\sin\beta - \sigma t)]}\right], \tag{5}$$

where $K = 2\pi/\bar{L} = \sigma^2/g$ is the wave-number, σ is the frequency, $\bar{L}$ is the wavelength and g is the gravitational constant. Using (5), the incident wave height is calculated from (3) as,

$$\bar{\eta}_w(\bar{x}, \bar{z}, t) = \mathrm{Re}[\bar{\eta}_w^0 e^{i(K\bar{x}\cos\beta + K\bar{z}\sin\beta - \sigma t)}], \tag{6}$$

where $\bar{\eta}_w^0$ is the complex amplitude of the incident wave.

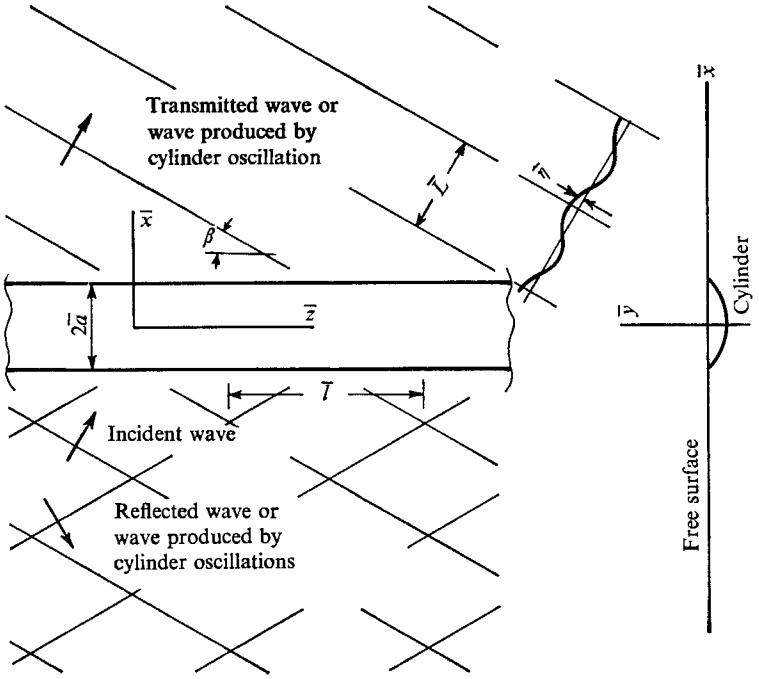

FIGURE 1. Definition sketch.

The cylinder is considered to be flexible and to deform in torsion about its $\bar{z}$ axis and its longitudinal axis is considered to deform sinusoidally in both the $\bar{x}$ and $\bar{y}$ direction. This displacement can be represented by the relationship

$$\bar{X}_i(\bar{z}, t) = \mathrm{Re}[\bar{x}_i^0 e^{i(K\bar{z}\sin\beta - \sigma t)}], \tag{7}$$

which describes a progressive wave travelling in the $\bar{z}$ direction, where $\bar{x}_i^0$ is the complex amplitude of oscillation and $i = 1$ corresponds to sway, $i = 2$ to heave and $i = 3$ to roll. In the case of roll $\bar{X}_3$ is not a length but an angle.

In considering the interaction of the incident wave with the fixed cylinder it is convenient to write Φ', which represents the velocity potential for the motion, as the sum,

$$\Phi' = \Phi_w + \Phi_4, \tag{8}$$

where Φ_w is the velocity potential for the incident wave and Φ_4 is called the scattering potential. The four velocity potentials which are involved in the present problem are, then, defined as

Φ_1 = velocity potential for x oscillations, sway;

Φ_2 = velocity potential for y oscillations, heave;

Φ_3 = velocity potential for θ oscillations, roll;

Φ_4 = velocity potential for scattering of the incident wave.

The boundary-value problems associated with the four velocity potentials, Φ_i $(i = 1, 2, 3, 4)$, are all similar; for all four problems Φ_i must satisfy the Laplace equation in the fluid region and the free surface boundary condition, equation (4), on $\bar{y} = 0$. Also, at a large distance from the cylinder the disturbances must become outgoing regular waves. This condition can be stated as,

$$\Phi_i(\bar{x}, \bar{y}, \bar{z}, t) \to \mathrm{Re}[C_i e^{[K\bar{y} \pm i(K\bar{x}\cos\beta + K\bar{z}\sin\beta - \sigma t]}], \quad \bar{x} \to \pm\infty, \tag{9}$$

where C_i is a constant.

The four boundary-value problems differ only in the kinematic boundary conditions to be applied on the surface of the cylinder. This boundary condition expresses the requirement that the fluid velocity normal to the surface must equal the velocity of the cylinder normal to itself. This gives:

$$\begin{aligned}
\Phi_{1\bar{n}} &= n_x \,\mathrm{Re}[-i\sigma\bar{x}_1^0 e^{-i(\sigma t - K\bar{z}\sin\beta)}],\\
\Phi_{2\bar{n}} &= n_y \,\mathrm{Re}[-i\sigma\bar{x}_2^0 e^{-i(\sigma t - K\bar{z}\sin\beta)}],\\
\Phi_{3\bar{n}} &= (\bar{x}n_y - \bar{y}n_x)\,\mathrm{Re}[-i\sigma\bar{x}_3^0 e^{-i(\sigma t - K\bar{z}\sin\beta)}],\\
\Phi_{4\bar{n}} &= \mathrm{Re}\left[-\frac{gK\eta_w^0}{\sigma}(n_y + in_x\cos\beta)\, e^{[K\bar{y} + i(K\bar{x}\cos\beta + K\bar{z}\sin\beta - \sigma t)]}\right].
\end{aligned} \tag{10}$$

The fluid motion represented by Φ_i is periodic in time as well as the $\bar{z}$ co-ordinate. Thus, the velocity potential may be written in the form

$$\Phi_i(\bar{x}, \bar{y}, \bar{z}, t) = \mathrm{Re}[U_i(\bar{x}, \bar{y})\, e^{i(K\bar{z}\sin\beta - \sigma t)}] \quad (i = 1, 2, 3, 4) \tag{11}$$

and, also, U', which corresponds to Φ' in accordance with (11), is defined as

$$U'(\bar{x}, \bar{y}) = -i(g\bar{\eta}_0/\sigma)\, e^{K(\bar{y} + i\bar{x}\cos\beta)} + U_4(\bar{x}, \bar{y}). \tag{12}$$

In terms of U_i the boundary-value problem can be stated for $i = 1, 2, 3, 4$ as:

$$\left.\begin{aligned}
&\nabla^2 U_i(\bar{x}, \bar{y}) - (K^2\sin^2\beta)\, U_i(\bar{x}, \bar{y}) = 0 && \text{in the fluid region,}\\
&U_i(\bar{x}, 0)_{\bar{y}} - KU_i(\bar{x}, 0) = 0 && \text{outside the cylinder,}\\
&U_i(\bar{x}, \bar{y})_{\bar{n}} = \bar{h}_i(\bar{x}, \bar{y}) && \text{on the surface of the cylinder,}\\
&U_i(\bar{x}, \bar{y}) \to C_i e^{K(\bar{y} \pm i\bar{x}\cos\beta)} && \text{for } \bar{x} \to \pm\infty,
\end{aligned}\right\} \tag{13}$$

where

$$\begin{aligned}
\bar{h}_1 &= -i\sigma\bar{x}_1^0 n_x,\\
\bar{h}_2 &= -i\sigma\bar{x}_2^0 n_y,\\
\bar{h}_3 &= -\sigma\bar{x}_3^0(\bar{x}n_y - \bar{y}n_x),\\
\bar{h}_4 &= (ig\bar{\eta}_w^0 K/\sigma)(n_y + in_x\cos\beta)\, e^{K(\bar{y} + i\bar{x}\cos\beta)}
\end{aligned}$$

and $\bar{n} = \hat{\imath}n_x + \hat{\jmath}n_y + \hat{k}n_z$ is the unit normal vector on the surface of the cylinder.

Before proceeding to the solution of (13) it is convenient to introduce dimensionless variables into the problem. Using the cylinder half-beam the following dimensionless variables are defined:

$$\left.\begin{aligned}
x &= \bar{x}/\bar{a}, \quad x_1^0 = \bar{x}_1^0/\bar{a}, \quad \eta_w^0 = \bar{\eta}_w^0/\bar{a},\\
y &= \bar{y}/\bar{a}, \quad x_2^0 = \bar{x}_2^0/\bar{a}, \quad a = K\bar{a} = 2\pi\bar{a}/\bar{L} = \sigma^2\bar{a}/g,\\
z &= \bar{z}/\bar{a}, \quad x_3^0 = \theta^0, \quad \nu = a\sin\beta.
\end{aligned}\right\} \tag{14}$$

Also, the dimensionless variable, $V_i(x, y)$, is defined as

$$\frac{i\sigma U_i(x\bar{a}, y\bar{a})}{g x_i^0 \bar{a}} = aV_i(x, y) \quad (i = 1, 2, 3) \tag{15}$$

and

$$\frac{i\sigma U'(x\bar{a}, y\bar{a})}{g\eta^0 \bar{a}} = e^{a(y+ix\cos\beta)} - aV_4(x, y). \tag{16}$$

The shape of the cross-section of the cylinder can be defined, in dimensionless form, as

$$Y(x) = \epsilon S(x), \tag{17}$$

where the parameter ϵ = draft/half-beam and $S(x)$ has the properties denoted in figure 2.

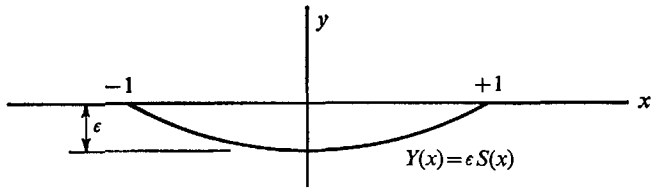

FIGURE 2. Cylinder cross-sectional shape. $S(x) = S(-x)$, $S(1) = S(-1) = 0$, $S(0) = -1$.

With the definitions introduced in (14), (15), (16) and (17) the boundary-value problem, (13), can be re-stated in concise dimensionless form as follows:

$$\left.\begin{aligned} &\nabla^2 V_i(x, y) - \nu^2 V_i(x, y) = 0 && \text{outside the cylinder and } y \leqslant 0,\\ &V_i(x, 0)_y - aV_i(x, 0) = 0 && \text{for } |x| \geqslant 1,\\ &V_i(x, y)_n = h_i(x, y) && \text{on } y = \epsilon S(x),\\ &V_i(x, y) \to C_i e^{a(y \pm ix\sqrt{(1-\nu^2/a^2)})} && (x \to \pm\infty), \end{aligned}\right\} \tag{18a–d}$$

where

$$h_1 = -\epsilon S'(x)\sqrt{\left(\frac{1}{1-\epsilon^2 S'^2(x)}\right)},$$

$$h_2 = \sqrt{\left(\frac{1}{1+\epsilon^2 S'^2(x)}\right)},$$

$$h_3 = x\sqrt{\left(\frac{1}{1+\epsilon^2 S'^2(x)}\right)} + \epsilon^2 S(x) S'(x)\sqrt{\left(\frac{1}{1-\epsilon^2 S'^2(x)}\right)},$$

$$h_4 = \left[\sqrt{\left(\frac{1}{1+\epsilon^2 S'^2(x)}\right)} - i\epsilon S'(x)\sqrt{\left(\frac{1-\nu^2/a^2}{1-\epsilon^2 S'^2(x)}\right)}\right] e^{a(\epsilon S(x) + ix\sqrt{(1-\nu^2/a^2)})}.$$

The solution V_i of the above-defined boundary-value problem is a function of the three dimensionless parameters ϵ, a and ν. ϵ reflects the draft/beam ratio, a the ratio of the cylinder size to wavelength and ν the angle that the wave crests make with the cylinder axis; $\nu = 0$ corresponds to the two-dimensional problem.

For arbitrary values of the three parameters involved, the solution of the boundary-value problem stated in (18) is difficult. To make some headway, however, one can limit consideration to certain limiting values of the parameters involved. In the present treatment small values of the draft/beam ratio

are considered by use of a procedure similar to that of MacCamy (1961). Accordingly, one can assume that the solution can be expanded in powers of ϵ as

$$V_i(x, y; \epsilon) = V_{i_0}(x, y) + \epsilon V_{i_1}(x, y) + \epsilon^2 V_{i_2}(x, y) + \ldots. \tag{19}$$

Likewise, the functions, h_i, can be expanded in a Taylor series about $\epsilon = 0$. Then, if these series representations are substituted into the boundary-value problem, (18), and coefficients of like powers of ϵ are collected, a series of new boundary-value problems is defined for each of the terms of the series in (19). The boundary-value problems for the first two terms of the series are listed below:

Zeroth-order problem

$$\left.\begin{aligned} &\nabla^2 V_{i_0}(x, y) - \nu^2 V_{i_0}(x, y) = 0 \quad (y \leqslant 0), \\ &V_{i_0}(x, 0)_y - a V_{i_0}(x, 0) = 0 \quad (|x| > 1), \\ &V_{i_0}(x, 0)_y = h_{i_0}(x) \quad (|x| \leqslant 1), \\ &V_{i_0}(x, y) \to C_{i_0} e^{a(y \pm ix\sqrt{(1-\nu^2/a^2)})} \quad (x \to \pm\infty), \end{aligned}\right\} \tag{20a–d}$$

where

$$\begin{aligned} h_{1_0}(x) &= 0, \\ h_{2_0}(x) &= 1, \\ h_{3_0}(x) &= x, \\ h_{4_0}(x) &= e^{iax\sqrt{(1-\nu^2/a^2)}}. \end{aligned}$$

First-order problem

$$\left.\begin{aligned} &\nabla^2 V_{i_1}(x, y) - \nu^2 V_{i_1}(x, y) = 0 \quad (y \leqslant 0), \\ &V_{i_1}(x, 0)_y - a V_{i_1}(x, 0) = 0 \quad (|x| > 1), \\ &V_{i_1}(x, 0)_y = h_{i_1}(x) + S'(x) V_{i_0}(x, 0)_x - \nu S(x) V_{i_0}(x, 0) + S(x) V_{i_0}(x, 0)_{xx} \quad (|x| \leqslant 1), \\ &V_{i_1}(x, y) \to C_{i_1} e^{a(y \pm ix\sqrt{(1-\nu^2/a^2)})} \quad (x \to \pm\infty), \end{aligned}\right\} \tag{21a–d}$$

where

$$\begin{aligned} h_{1_1}(x) &= -S'(x), \\ h_{2_1}(x) &= 0, \\ h_{3_1}(x) &= 0, \\ h_{4_1}(x) &= (aS(x) + iS'(x)\sqrt{(1-\nu^2/a^2)})\, e^{iax\sqrt{(1-\nu^2/a^2)}}. \end{aligned}$$

It is interesting to note that the problems stated above are of the same type; both have the same differential equation, free surface boundary condition and asymptotic condition. The only difference lies in the form of the right side of condition (*c*). In fact, the problems for all of the terms, V_{i_n}, are similar and differ only in the form of the right side of (*c*).

The remainder of this paper will deal with the solution of the zeroth-order problem, i.e. the problem stated in (20). This problem corresponds to zero-draft, that is, a horizontal strip lying on the free surface. For convenience sake, the subscript '0' will be dropped and consideration will be limited to $i = 2, 3, 4$ since Φ_1, corresponding to the velocity potential for sway, is trivial because no disturbance is caused by a cylinder of zero-draft oscillating in this mode. The

boundary-value problem in question for zero-draft and $i = 2, 3, 4$ can be stated as:

$$\left.\begin{aligned} &\nabla^2 V_i(x,y) - \nu^2 V_i(x,y) = 0 \quad (y \leqslant 0), \\ &V_i(x,0)_y - a V_i(x,0) = 0 \quad (|x| > 1), \\ &V_i(x,0)_y = h_i(x) \quad (|x| \leqslant 1), \\ &V_i(x,y) \to C_i\, e^{a(y \pm ix\sqrt{(1-\nu^2/a^2)})} \quad (x \to \pm\infty), \end{aligned}\right\} \tag{22a–d}$$

where

$$\begin{aligned} h_2 &= 1, \\ h_3 &= x, \\ h_4 &= e^{iax\sqrt{(1-\nu^2/a^2)}}. \end{aligned}$$

Green's function

The solution to the problem stated in (22) can be formulated in terms of Green's function. One can proceed to this formulation by applying the Green's theorem to the region occupied by the fluid as depicted in figure 3. $V_i(x,y)$ and the Green's function, $G(x,y;\xi,\eta)$, are chosen as subjects for application of the Green's reciprocal theorem yielding

$$\begin{aligned} &\iint_R [\nabla^2 V_i(x,y) - \nu^2 V_i(x,y)]\, G(x,y;\xi,\eta)\, dx\, dy \\ &\qquad - \iint_R [\nabla^2 G(x,y;\xi,\eta) - \nu^2 G(x,y;\xi,\eta)]\, V_i(x,y)\, dx\, dy \\ &= \oint_{S_s+S_b+S_c+S_\infty} \left[G(x,y;\xi,\eta) \frac{\partial V_i(x,y)}{\partial n} - V_i(x,y) \frac{\partial G(x,y;\xi,\eta)}{\partial n} \right] dS, \end{aligned} \tag{23}$$

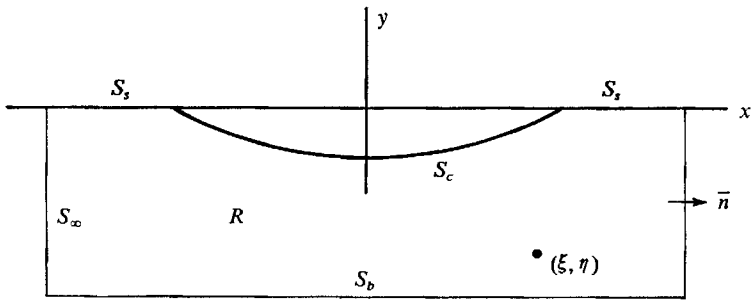

FIGURE 3. Definition sketch for application of Green's theorem.

where (ξ,η) denotes some point interior to the region, R, and n denotes the direction of the outward normal at the surface of the region. If $G(x,y;\xi,\eta)$ is selected such that it satisfies the following differential equation

$$\nabla^2 G(x,y;\xi,\eta) - \nu^2 G(x,y;\xi,\eta) = \delta(x-\xi)\,\delta(y-\eta), \tag{24}$$

where $\delta(x)$ is the Dirac delta function, then, (23) reduces to

$$V_i(\xi,\eta) = \oint_{S_s+S_b+S_c+S_\infty} \left[G(x,y;\xi,\eta) \frac{\partial V_i(x,y)}{\partial n} - V_i(x,y) \frac{\partial G(x,y;\xi,\eta)}{\partial n} \right] dS, \tag{25}$$

since $V_i(x, y)$ satisfies the equation

$$\nabla^2 V_i(x, y) - \nu^2 V_i(x, y) = 0.$$

If, further, $G(x, y; \xi, \eta)$ is required to satisfy the free surface boundary condition for all values of x and the radiation condition as indicated in (22*b* and *d*), the integrals in (25) vanish over all of the surfaces except the surface of the cylinder, S_c, yielding

$$V_i(\xi, \eta) = \oint_{S_c} \left(\frac{\partial V_i}{\partial n}(x, y) - aV_i(x, y)\right) G(x, y;\ \xi, \eta)\, dS - \oint_{S_c} \left(\frac{\partial G}{\partial n}(x, y; \xi, \eta) - G(x, y; \xi, \eta)\right) V_i(x, y)\, dS.$$

Restricting this further to zero draft, the second integral vanishes since G satisfies the free surface boundary condition,

$$G(x, 0;\ \xi, \eta)_y - aG(x, 0;\ \xi, \eta) = 0$$

as previously noted. Thus, for the zero-draft cylinder (upon reversing the roles of x, y and ξ, η) the solution to the boundary-value problem, (22), may be written as

$$V_i(x, y) = \int_{-1}^{+1} f_i(\xi)\, G(x, y; \xi)\, d\xi, \tag{26}$$

where the distribution function, f_i, is defined as

$$f_i(x) = V_i(x, 0)_y - aV_i(x, 0), \quad \text{for} \quad |x| \leqslant 1. \tag{27}$$

In developing (26) a number of requirements were placed on the Green's function. In summary these are:

$$\left.\begin{aligned} &\nabla^2 G(x, y; \xi) - \nu^2 G(x, y; \xi) = \delta(x - \xi)\, \delta(y), \\ &G(x, 0; \xi)_y - aG(x, 0; \xi) = 0 \quad \text{for all } x, \\ &G(x, y; \xi) \to C\, e^{a(y \pm ix\sqrt{(1 - \nu^2/a^2)})} \quad (x \to \pm\infty). \end{aligned}\right\} \tag{28a–c}$$

Equations (28*a–c*) define a boundary-value problem for the Green's function which is similar to, but simpler than, the original problem for V_i. According to (28), the Green's function must satisfy the basic differential equation of the problem, except at the point $(\xi, 0)$, the free surface boundary condition for all values of x (rather than for $|x| \geqslant 1$ as was required of V_i) and must represent an outgoing regular wave at $x \to \pm\infty$.

The solution to (28) for the Green's function can be obtained by use of the Fourier and Laplace transforms applied to the $x - \xi$ and y variables, respectively. The result of this procedure yields the Green's function,

$$G(x - \xi, y) = \frac{1}{2\pi} \int_{-\infty}^{+\infty} \frac{e^{i(x-\xi)}\, e^{ky}\, d\zeta}{(k - a)}, \tag{29}$$

(where $k = \sqrt{(\zeta^2 + \nu^2)}$) which satisfies (28*a*) and (28*b*) and approaches zero for $y \to -\infty$ as required by (28*c*). However, this integral deserves further consideration since it possesses singularities at $\zeta = \pm\sqrt{(a^2 - \nu^2)}$ and its satisfaction of the radiation boundary condition for $x - \xi \to \pm\infty$ has yet to be tested.

To examine the Green's function further the infinite integral in (29) can be expressed as one segment of a contour integral in the upper half ζ plane. If the contour indicated in figure 4 is taken for $x-\xi > 0$ where the branch cut extending from $i\nu$ to $i\infty$ is observed, the resulting expression will satisfy (28c) at $x-\xi \to +\infty$. A reflexion of this contour into the lower half ζ plane will result in a similar expression for G for $x-\xi < 0$, differing only in the sign of $x-\xi$. Thus, placing

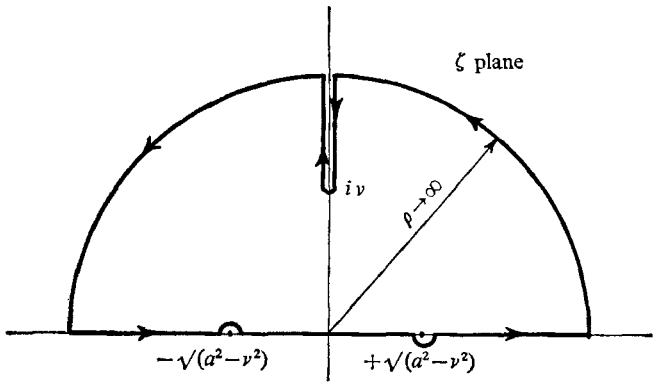

FIGURE 4. Integration path for $(x-\xi) > 0$.

absolute value signs about $x-\xi$ occurring in these expressions yields the following form for the Green's function which satisfies all of the conditions stated in (28) for all values of $x-\xi$:

$$G(x-\xi,y) = \frac{1}{\pi}\int_{\nu}^{\infty} \frac{[\sqrt{(\eta^2-\nu^2)}\cos(\sqrt{(\eta^2-\nu^2)}y) + a\sin(\sqrt{(\eta^2-\nu^2)}y)]}{a^2+\eta^2-\nu^2} e^{-|x-\xi|\eta}\, d\eta$$
$$+ i[a/\sqrt{(a^2-\nu^2)}]\, e^{i\sqrt{(a^2-\nu^2)}|x-\xi|} e^{ay}. \quad (30)$$

Now that the Green's function has been obtained, we turn to the evaluation of the distribution function, $f_i(x)$, by application of the kinematic boundary condition on the surface of the cylinder. Substituting (26) and (22c) into (27) yields the following integral equation for $f_i(x)$:

$$f_i(x) + a\int_{-1}^{+1} f_i(\xi)\, G(x-\xi,0)\, d\xi = h_i(x) \quad (|x| \leqslant 1). \quad (31)$$

The integral equation (31) can be solved by numerical methods but in order to do so it is necessary to evaluate its kernel on $y = 0$. To this end (30) is evaluated on $y = 0$ and the integral term occurring therein is arranged in parts yielding:

$$G(x-\xi,0) = -\frac{1}{\pi}\int_0^1 \frac{e^{-|x-\xi|\nu u}u\, du}{u^2+a^2/\nu^2-1} - \frac{1}{\pi}\int_1^{\infty} \frac{(u-\sqrt{(u^2-1)})}{u^2+a^2/\nu^2-1} e^{-|x-\xi|\nu u}\, du$$
$$+ \frac{1}{\pi}\int_0^{\infty} \frac{e^{-|x-\xi|\nu u}\, u\, du}{u^2+a^2/\nu^2-1} + i\frac{a}{\sqrt{(a^2+\nu^2)}} e^{i\sqrt{(a^2-\nu^2)}|x-\xi|}. \quad (32)$$

The third integral term in the above expression is given by Gröbner & Hofreiter (1966) as

$$\int_0^\infty \frac{e^{-|x-\xi|\nu u}u\,du}{u^2+a^2/\nu^2-1} = \tfrac{1}{2}\pi \sin\left(\sqrt{(a^2-\nu^2)}|x-\xi|\right) - \sin\left(\sqrt{(a^2-\nu^2)}|x-\xi|\right)\mathrm{Si}\left(\sqrt{(a^2-\nu^2)}|x-\xi|\right) - \cos\left(\sqrt{(a^2-\nu^2)}|x-\xi|\right)\mathrm{Ci}\left(\sqrt{(a^2-\nu^2)}|x-\xi|\right),$$

where Si and Ci denote the integral sine and integral cosine, respectively. The complete Green's function is, therefore, given by

$$G(x-\xi,0) = \frac{1}{\pi}\left[-\int_0^1 \frac{e^{-|x-\xi|\nu u}u\,du}{u^2+a^2/\nu^2-1} - \int_1^\infty \frac{(u-\sqrt{(u^2-1)})e^{-|x-\xi|\nu u}}{u^2+a^2/\nu^2-1}\,du + \pi\left(\frac{1}{2}-\frac{a}{\sqrt{(a^2-\nu^2)}}\right)\sin\left(\sqrt{(a^2-\nu^2)}|x-\xi|\right) - \sin\left(\sqrt{(a^2-\nu^2)}|x-\xi|\right)\mathrm{Si}\left(\sqrt{(a^2-\nu^2)}\,|x-\xi|\right) - \cos\left(\sqrt{(a^2-\nu^2)}|x-\xi|\right)\mathrm{Ci}\left(\sqrt{(a^2-\nu^2)}|x-\xi|\right) + \ln|x-\xi| + i\frac{\pi a}{\sqrt{(a^2-\nu^2)}}\cos\left(\sqrt{(a^2-\nu^2)}|x-\xi|\right)\right] - \frac{1}{\pi}\ln|x-\xi|. \tag{33}$$

The desired result has been obtained; the Green's function which is the kernel of the integral equation, (31), has been arranged in a form which can be numerically evaluated on $y = 0$. The two remaining integrals in (33) must, however, be evaluated by numerical integration but this is not a particularily difficult task since the first integral term has finite limits of integration and the second, although containing an infinite upper limit, is rapidly convergent.

It is noted that Ci(z), in (33), is singular like ln(z) as $z \to 0$. Thus, as $|x-\xi| \to 0$ the integral cosine term will cancel the $\ln|x-\xi|$ term so that the whole expression within brackets will be regular while the last term will provide a logarithmic singularity at $|x-\xi| = 0$.

Numerical analysis

The essential problem remaining in the original boundary-value problem is the solution of the integral equation, (31). Since the kernel of that equation is extremely complex it is natural to attempt a numerical solution. To that end the interval $x = -1$ to $+1$ is divided into m elements of length $\Delta x = 2/m$ as indicated in figure 5. The value of x_i is then considered to lie at the centre of the ith element and if we denote by f_{n_i} the value of f_n evaluated at x_i ($n = 2, 3, 4$ corresponds to roll, heave and scattering, respectively) the integral equation may be written as

$$f_{n_j} + a\int_{-1}^{+1} f_n(t)\,G(x_j-t,0)\,dt = h_{n_j} \quad (j = 1, 2, 3, \ldots, m). \tag{34}$$

Furthermore, if we use the value of f_{n_i} to represent f_n over that element, we can approximate (34), further, by

$$f_{n_j} + af_{n_i}\int_{x_i-\Delta x/2}^{x_i+\Delta x/2} G(|x_j-t|,0)\,dt = h_{n_j}.$$

This equation can be written more conveniently in the form of a matrix equation as

$$f_{nj}+f_{ni}H_{ij}=h_{nj}, \tag{35}$$

where the matrix elements, H_{ij}, are given by

$$H_{ij}=a\int_{x_i-\Delta x/2}^{x_i+\Delta x/2} G(|x_j-t|,0)\,dt. \tag{36}$$

Thus, the solution of the integral equation, (31), reduces to the solution of the system of linear equations, or matrix equation, given by (35), for the column matrix, $[f_n]$.

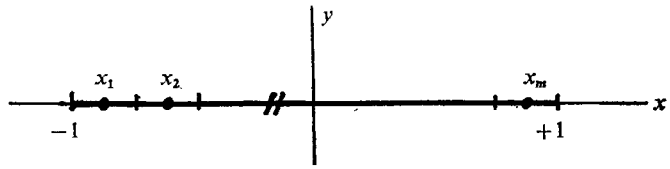

FIGURE 5. Numerical scheme.

Except for the case of $i=j$, (36) can be approximated by

$$H_{ij}=aG(|x_j-x_i|,0)\,\Delta x \quad (i\neq j), \tag{37}$$

where $G(|x_j-x_i|)$ is evaluated by use of (33). The two integral terms occurring in (33) must be evaluated by numerical integration by replacing the infinite upper limit in the second integral by a suitably large finite number. The error involved in this approximation is discussed in appendix A.

When $i=j$ the Green's function is logarithmically singular and, consequently, the approximation of the integral given by (37) cannot be used. Instead, we must carry out the integration of the logarithmic part analytically as indicated in (36). Although $\ln|x_j-t|$ is infinite at $t=x_j$, its integral over the element is finite and easily evaluated. The regular term in (33) can, however, be evaluated by the approximate relationship, (37).

In utilizing the approximation given by (37) for $i\neq j$ there arises a question of accuracy. Certainly when G is regular H_{ij}, as obtained by (37), converges to that given by (36) as $2/m=\Delta x\to 0$. However, when the logarithmic term occurring in the integrand is evaluated by (37) at $i=j\pm 1$ it is not at all obvious that this result converges to that given by (36) as $\Delta x\to 0$. Thus, appendix B has been included to show that the use of (37) is justified even for the logarithmic term in G at the most critical condition of $i=j\pm 1$.

A digital computer program was developed to carry out the numerical calculations for the results presented in this paper. The integrals occurring in (33) were evaluated by use of Simpson's rule, replacing the infinite upper limit in the second integral by the value of 50. In appendix A, it is shown that this approximation leads to an error of less than 0·02 percent when compared to the complete infinite integral term in (30) evaluated at $y=0$.

The value of $m=40$ was used for purposes of calculating the numerical results presented in the figures. This made $[H]$ a 40×40 matrix and $[f_n]$ and $[h_n]$ 40 element column matrices. Preliminary to this, however, results were calculated

using $m = 20$. The discrepancy between the two sets of results was slight, becoming significant only at large values of a (say, $a > 6{\cdot}0$ at $\nu = 0$) and small values of ν/a. We note that this behaviour of the numerical results, however, is not surprising since the wavelength of the fluctuations of the Green's function (which must be large compared to the subdivision length, $2/m$, for good accuracy) is proportional to

$$\frac{1}{a\sqrt{(1-\nu^2/a^2)}}.$$

Accordingly, the fluctuation wavelength decreases with a but increases with ν/a, making the two-dimensional case the most critical with respect to this limitation.

We remark that MacCamy (1964), using a numerical procedure similar to the present one, also found very little difference between his results obtained using $m = 12$ and $m = 36$ for the two-dimensional case of the present problem for heave.

Physical quantities

In order to determine the forces and moments acting on the cylinder due to the fluid motion induced by the incident wave train or by the motion of the cylinder itself, it is necessary to evaluate the pressure on the surface of the cylinder and then calculate the net effect of the pressure distribution.

If the dynamic pressure is defined as

$$\bar{\pi} = P + \rho g \bar{y},$$

where P is the static pressure, Bernoulli's equation gives the pressure in terms of the time derivative of the velocity potential as

$$\bar{\pi} = -\rho \Phi_t,$$

provided the velocity squared terms appearing therein are neglected. Taking account of the relationship between Φ and V through (11), (12), (15) and (16) we obtain the pressure on the surface of the cylinder as

$$\bar{\pi}_i(x, 0, z, t) = \rho g \bar{a}\, \mathrm{Re}\,[x_i^0 a V_i(x, 0)\, e^{i(\nu z - \sigma t)}] \quad (i = 2, 3) \tag{38}$$

and

$$\bar{\pi}'(x, 0, z, t) = \rho g \bar{a}\, \mathrm{Re}\,[\eta_w^0 (h_4(x) - a V_4(x, 0))\, e^{i(\nu z - \sigma t)}], \tag{39}$$

where $\bar{\pi}'$ is associated with Φ' (that is, $\bar{\pi}'$ is the pressure due to the interaction of the incident wave with the fixed cylinder) and $\bar{\pi}_i$ is the pressure due to heave and roll in still water. Using equation (27), the dimensionless pressure amplitude on the surface of the cylinder can be written as

$$\left| \frac{(\bar{\pi}_i)_{\max}}{\rho g \bar{a} x_i^0} \right| = |h_i(x) - f_i(x)| \quad (i = 2, 3) \tag{40}$$

and

$$\left| \frac{(\bar{\pi}')_{\max}}{\rho g \bar{a} \eta_w^0} \right| = |f_4(x)|. \tag{41}$$

The pressure amplitude distributions obtained from these equations are plotted in figures 6–10. The two dimensionless parameters given in (40) and (41) can be

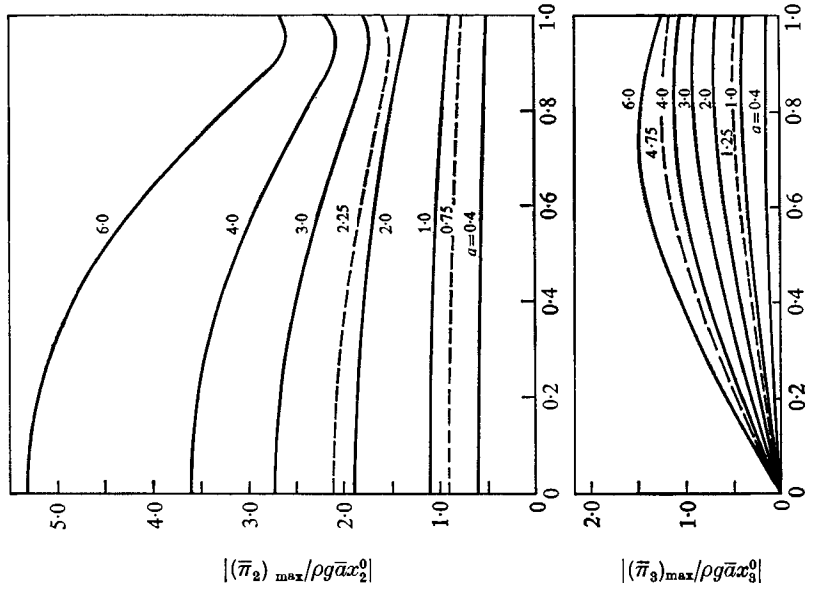

FIGURE 6. Pressure amplitude in heave and roll for $\nu = 0$. – – –, MacCamy (1964).

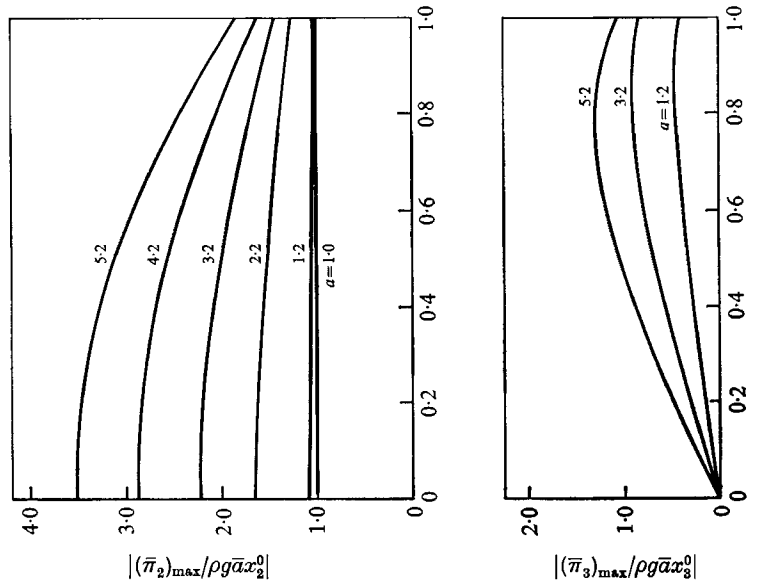

FIGURE 7. Pressure amplitude in heave and roll for $\nu = 1{\cdot}0$.

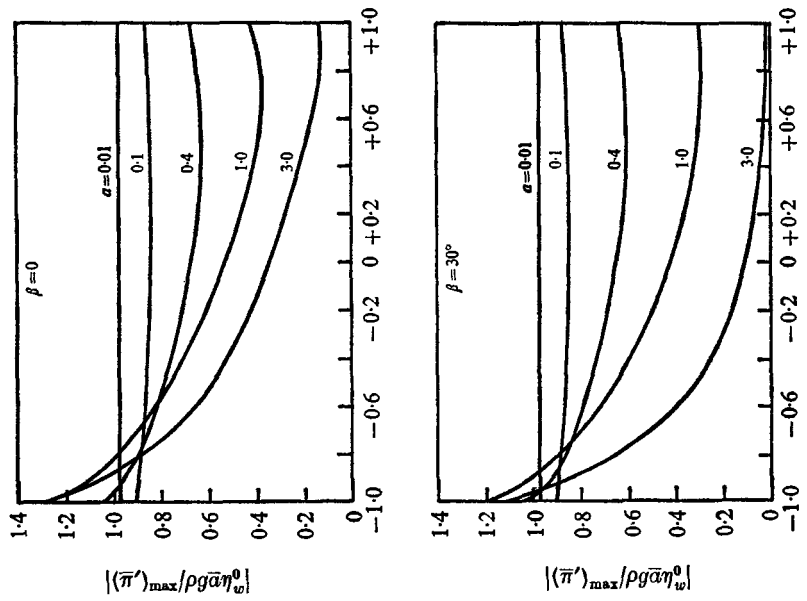

FIGURE 9. Pressure amplitude distribution due to wave interaction with cylinder fixed.

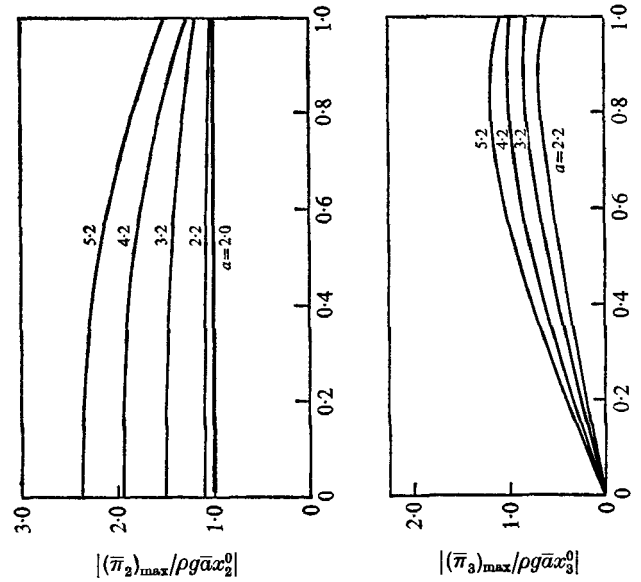

FIGURE 8. Pressure amplitude in heave and roll for $\nu = 2{\cdot}0$.

considered to be the ratio of the pressure in feet of water to the magnitude of the oscillation $\bar{a}x_i^0$ for $i = 2$ and 3 and the pressure in feet of water to the wave height, $\bar{a}\eta_w^0$, respectively.

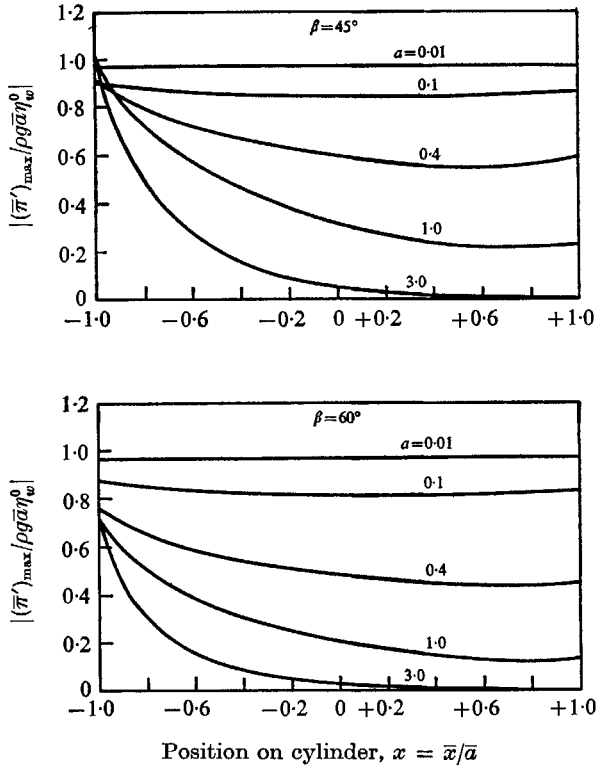

FIGURE 10. Pressure amplitude distribution due to wave interaction with cylinder fixed.

The forces and moments due to the incident wave interaction with the fixed cylinder are obtained by numerical quadrature involving the pressure and the surface of the cylinder. The wave force and moment are, therefore, given by

$$\bar{F}_i = (\bar{a} \text{ or } \bar{a}^2)\int_{S_c} \bar{\pi}' h_i \, dS, \quad dS = d\bar{S}/\bar{a},$$

where $\bar{a}$ is used in the case of a force, (i.e.) when $i = 2$, and $\bar{a}^2$ in the case of a moment, when $i = 3$. Substituting for pressure from (39) and using (27) gives

$$\bar{F}_i = \text{Re}\left[\rho g \eta_w^0 \bar{a}(\bar{a} \text{ or } \bar{a}^2)\left(\int_{-1}^{+1} h_i(x) f_4(x)\, dx\right) e^{i(\nu z - \sigma t)}\right].$$

In terms of the force (or moment) coefficient, C_i, which is defined as

$$C_i = \frac{|(\bar{F}_i)_{\max}|}{|\rho g \eta_w^0 \bar{a}(\bar{a} \text{ or } \bar{a}^2)|},$$

we have

$$C_i = \left|\int_{-1}^{+1} h_i(x) f_4(x)\, dx\right|. \tag{42}$$

C_2 is the heave force coefficient and C_3 is the moment coefficient. These coefficients are plotted in figures 11 and 12, respectively.

The forces and moments associated with the motion of the cylinder are best represented in the form of added mass or moment of inertia and damping coefficients. These are coefficients of force (or moments) which are proportional to the acceleration and velocity, respectively. To develop these coefficients the

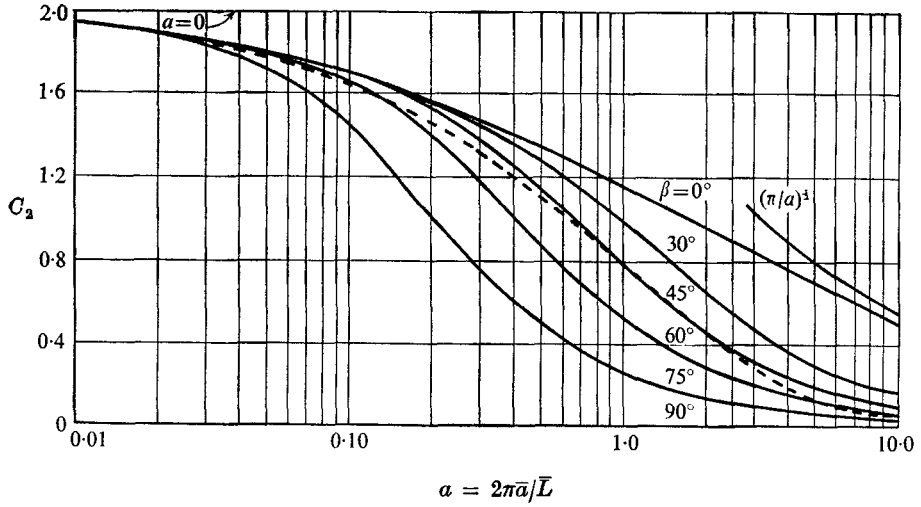

FIGURE 11. Heave force coefficient for wave interaction with cylinder fixed. – – –, circular cylinder, $\beta = 0°$, Dean & Ursell (1959).

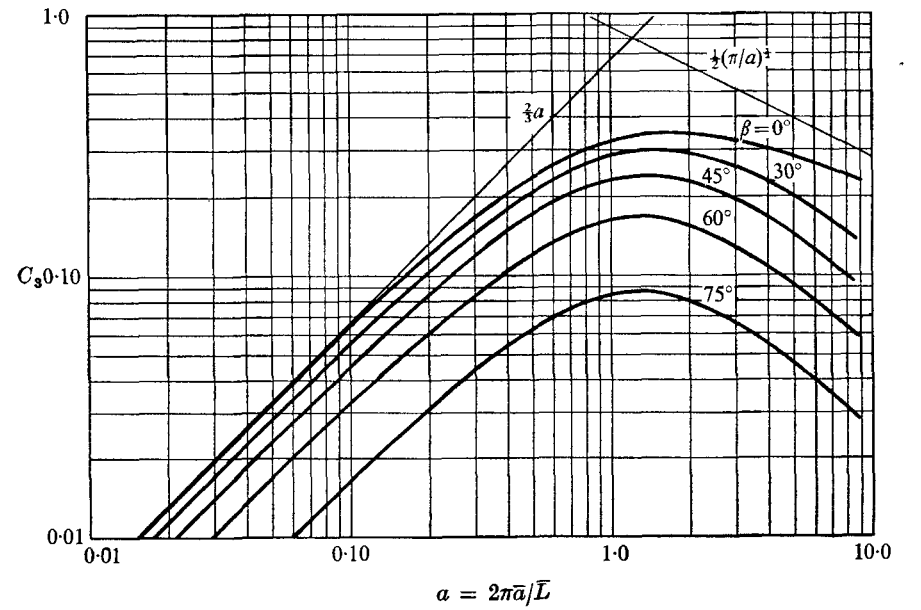

FIGURE 12. Moment coefficient for wave interaction with cylinder fixed.

ith component of force (or moment) per unit length of cylinder due to the jth component of motion of the cylinder is written as

$$\bar{F}_i = (\bar{a} \text{ or } \bar{a}^2) \int_{S_c} \bar{\pi}_j h_i \, dS,$$

where, again, $\bar{a}$ is used in the case of a force ($i = 2$) and $\bar{a}^2$ is used in the case of a moment ($i = 3$). Using (38) and (27) and noting that h_i is real gives

$$\bar{F}_i = \mathrm{Re}\left[\rho g x_j^0 \bar{a}(\bar{a} \text{ or } \bar{a}^2)\left(\int_{-1}^{+1} h_i(x)\,(h_j(x) - f_j(x))\,dx\right) e^{i(\nu z - \sigma t)}\right]. \tag{43}$$

The jth component of motion of the cylinder which gives rise to this ith component of force (or moment) is given by (7). Taking the derivative of this expression with respect to time gives the jth component of velocity as

$$\dot{\bar{X}}_j = (1 \text{ or } \bar{a}) x_j^0 \sigma \,\mathrm{Re}\,[-i\, e^{i(\nu z - \sigma t)}], \tag{44}$$

and the second derivative gives the jth component of acceleration,

$$\ddot{\bar{X}}_j = (1 \text{ or } \bar{a}) x_j^0 \sigma^2 \,\mathrm{Re}\,[-e^{i(\nu z - \sigma t)}], \tag{45}$$

where 1 is chosen when $\bar{X}_j$ is an angle, ($j = 3$), and $\bar{a}$ is chosen when $\bar{X}_j$ is a linear displacement, ($j = 2$). Furthermore, the force (or moment) can be divided into two components, one component proportional to the acceleration and one component proportional to the velocity as

$$\bar{F}_i = -\bar{M}_{ij} \ddot{\bar{X}}_j - \bar{N}_{ij} \dot{\bar{X}}_j \quad (\text{no sum on } j), \tag{46}$$

where $\bar{M}_{ij}$ and $\bar{N}_{ij}$ are added mass and damping factors, respectively. Using (44) and (45) we obtain

$$\bar{F}_i = \mathrm{Re}\,[\rho g x_j^0 \bar{a}(\bar{a} \text{ or } \bar{a}^2)(a M_{ij} + i a N_{ij}) e^{i(\nu z - \sigma t)}], \tag{47}$$

where the dimensionless added mass and damping coefficients are defined, respectively, as

$$M_{ij} = \frac{\bar{M}_{ij}(1 \text{ or } \bar{a})}{\rho \bar{a}^2 (\bar{a} \text{ or } \bar{a}^2)}, \tag{48}$$

$$N_{ij} = \frac{\bar{N}_{ij}(1 \text{ or } \bar{a})}{\rho \sigma \bar{a}^2 (\bar{a} \text{ or } \bar{a}^2)}. \tag{49}$$

Comparing (43) with (47) it is evident that the added mass and damping coefficients are given by

$$M_{ij} = \mathrm{Re}\left[(1/a)\int_{-1}^{+1} h_i(x)\,(h_j(x) - f_j(x))\,dx\right], \tag{50}$$

and

$$N_{ij} = \mathrm{Im}\left[(1/a)\int_{-1}^{+1} h_i(x)\,(h_j(x) - f_j(x))\,dx\right]. \tag{51}$$

Due to the symmetry of the cylinder with respect to the $x = 0$ plane, $M_{ij} = N_{ij} = 0$ for $i + j$. When $i = j$ the proper selection of (1 or $\bar{a}$) and ($\bar{a}$ or $\bar{a}^2$) has been made and the coefficients in their proper form are listed below:

$i = j = 2$; y component of force due to y motion (heave),
added mass coefficient, $M_{22} = \bar{M}_{22}/\rho\bar{a}^2$,
damping coefficient, $N_{22} = \bar{N}_{22}/\rho\sigma\bar{a}^2$.

$i = j = 3$; moment about the z axis due to θ motion (roll),
added moment of inertia coefficient, $M_{33} = \bar{M}_{33}/\rho\bar{a}^4$,
damping coefficient, $N_{33} = \bar{N}_{33}/\rho\sigma\bar{a}^2$.

The numerical results obtained for these coefficients are plotted in figures 13–16.

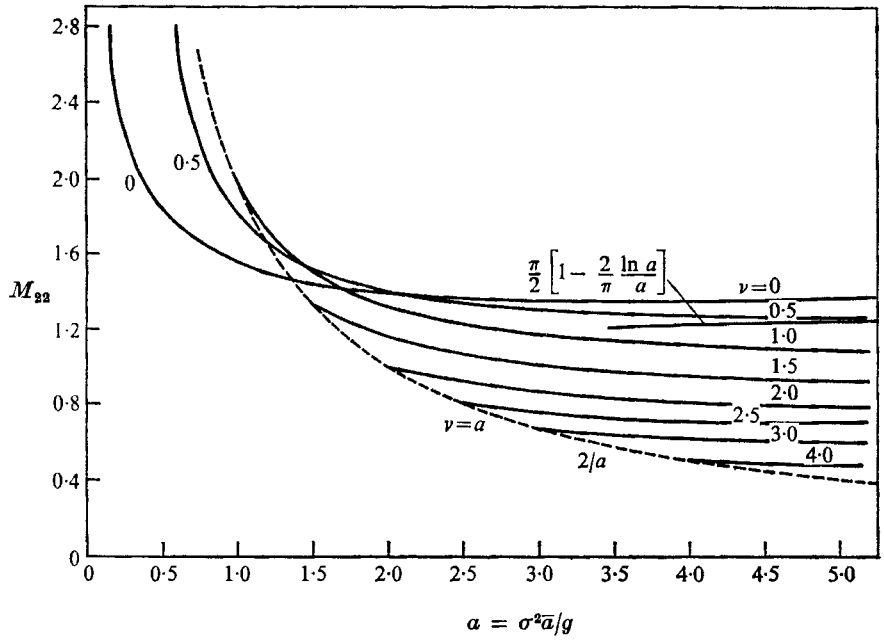

FIGURE 13. Added mass coefficient in heave.

Aside from the results already considered there are a group which may be termed 'far field' characteristics since they are obtained from the behaviour of the velocity potential at $x \to \pm\infty$. These include, for $i = 2$ and 3, the waves produced by the heaving and rolling motion of the cylinder and, for $i = 4$, the transmitted wave at $x \to +\infty$ and the reflected wave at $x \to -\infty$.

In order to calculate the height of the wave produced at $x \to \pm\infty$ we use the asymptotic form of (30) for $x \to \infty$ along with (26) to obtain the asymptotic form of V_i as

$$V_i(x, y) \sim \frac{i}{\sqrt{(1-\nu^2/a^2)}} e^{a(y+ix\sqrt{(1-\nu^2/a^2)})} \int_{-1}^{+1} f_i(\xi)\, e^{-i\xi a\sqrt{(1-\nu^2/a^2)}}\, d\xi, \quad x \to \infty. \tag{52}$$

From Bernoulli's equation the wave height is related to the velocity potential by

$$\bar{\eta} = -\frac{1}{g}\Phi_t, \tag{53}$$

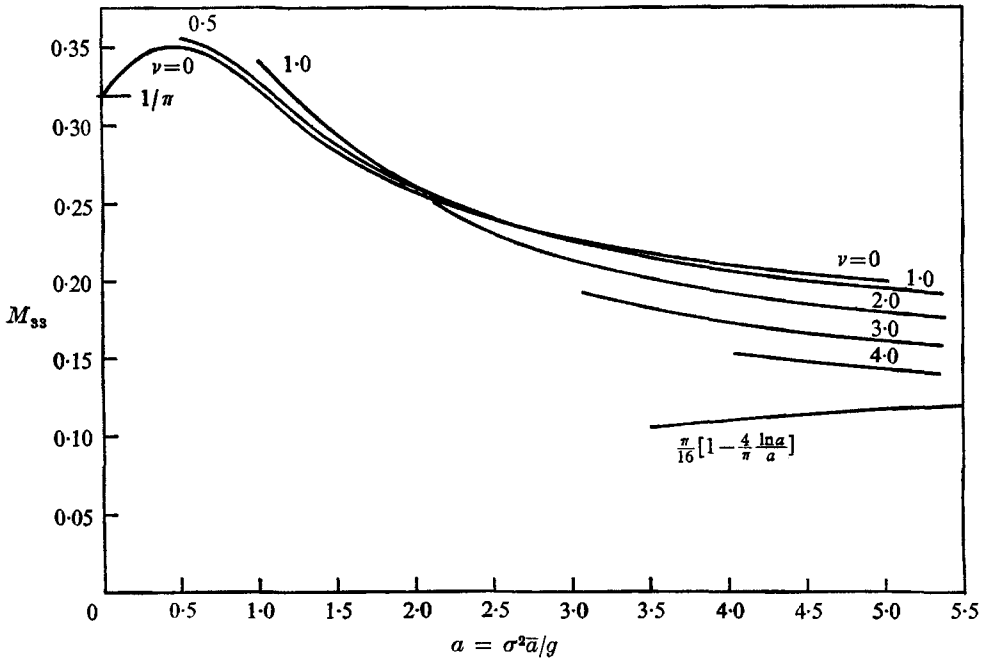

FIGURE 14. Added moment of inertia coefficient in roll.

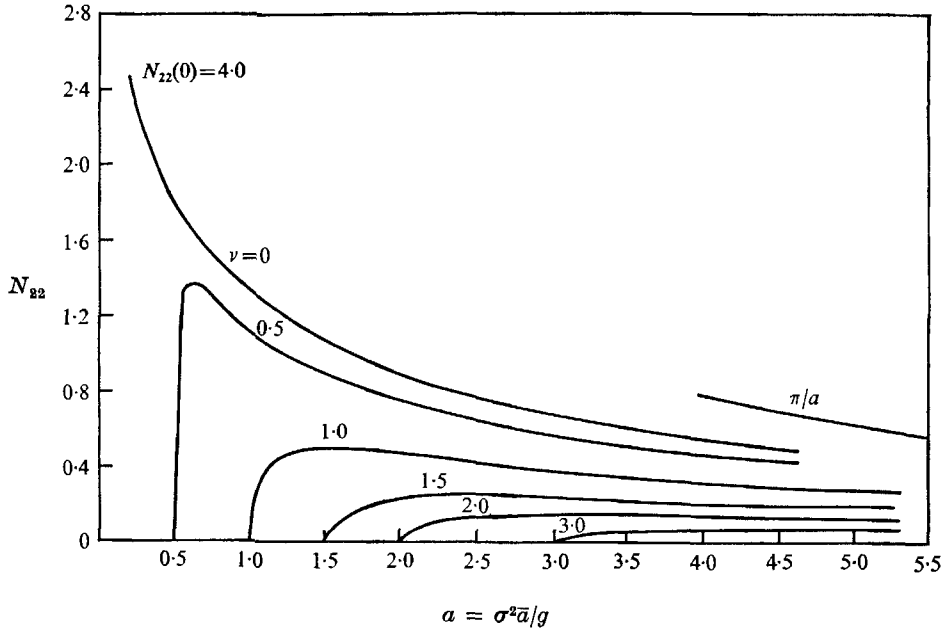

FIGURE 15. Damping coefficient in heave.

so that (52), (11) and (15) with (53) yield the wave height at $x \to \infty$ relative to the amplitude of the cylinder motion as

$$\left|\frac{\overline{\eta}_{\max}}{x_i^0 \overline{a}}\right| = \left|\frac{ia}{\sqrt{(1-\nu^2/a^2)}} \int_{-1}^{+1} f_i(\xi)\, e^{-i\xi a\sqrt{(1-\nu^2/a^2)}}\, d\xi\right|. \tag{54}$$

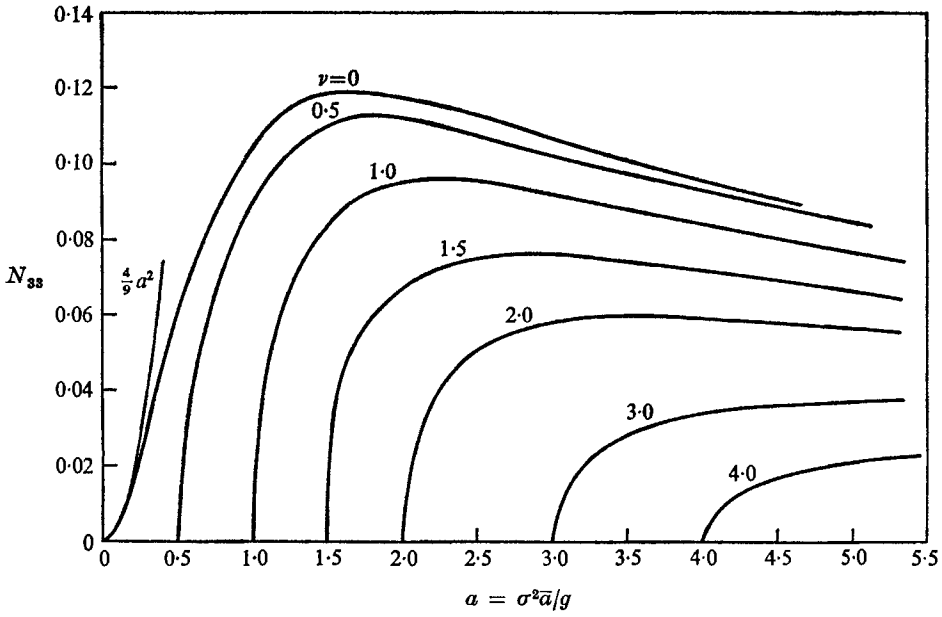

FIGURE 16. Damping coefficient in roll.

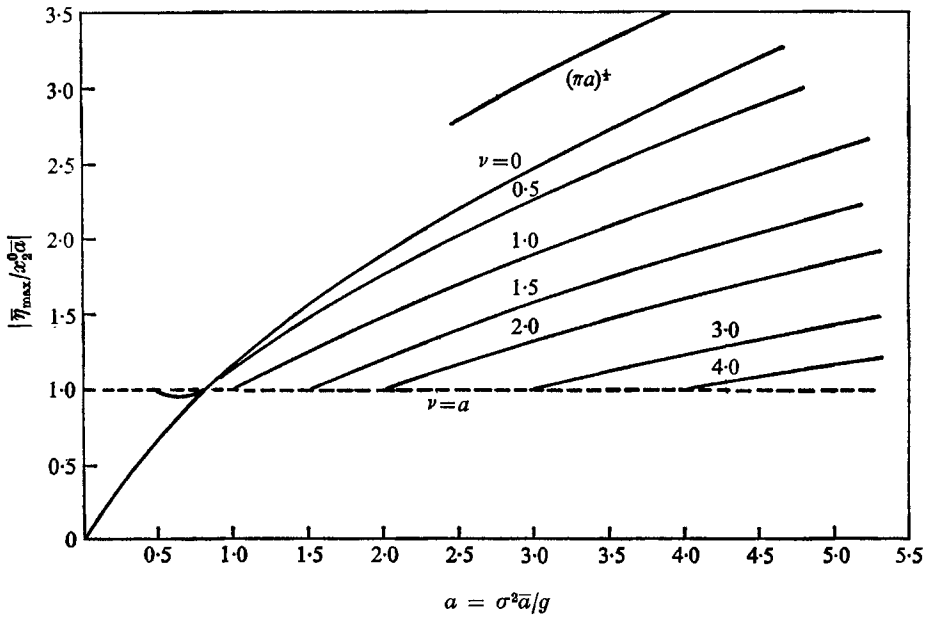

FIGURE 17. Wave height ratio in heave.

This parameter is called the 'wave height ratio' and is plotted in figures 17 and 18 for heave and roll, respectively.

For the case of the incident wave interaction with the fixed cylinder the pertinent 'far field' characteristics are the heights of the transmitted and reflected waves. The reflected wave height is obtained in a fashion similar to that of obtaining the wave height ratio by use of the asymptotic form of V_4 at $x \to -\infty$.

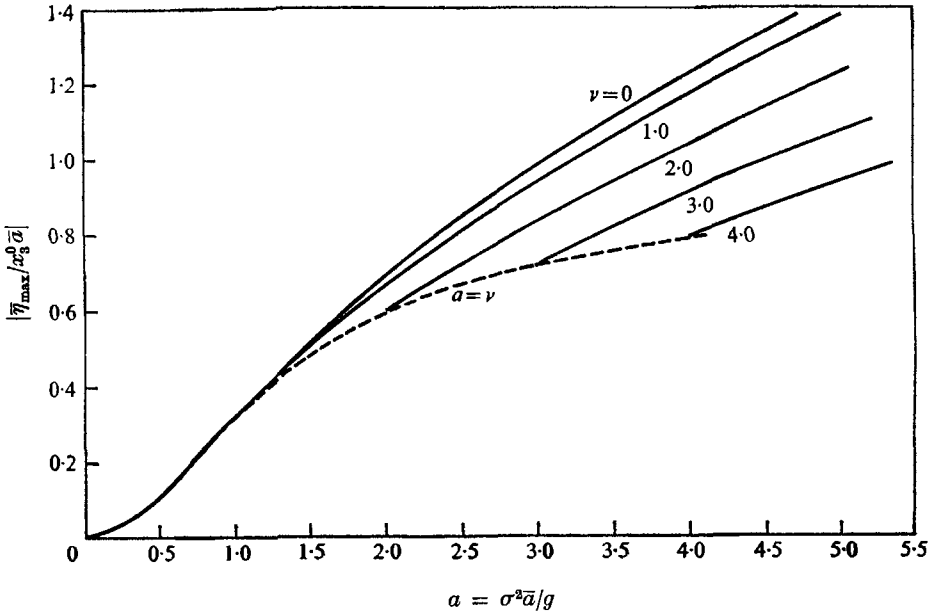

FIGURE 18. Wave height ratio in roll.

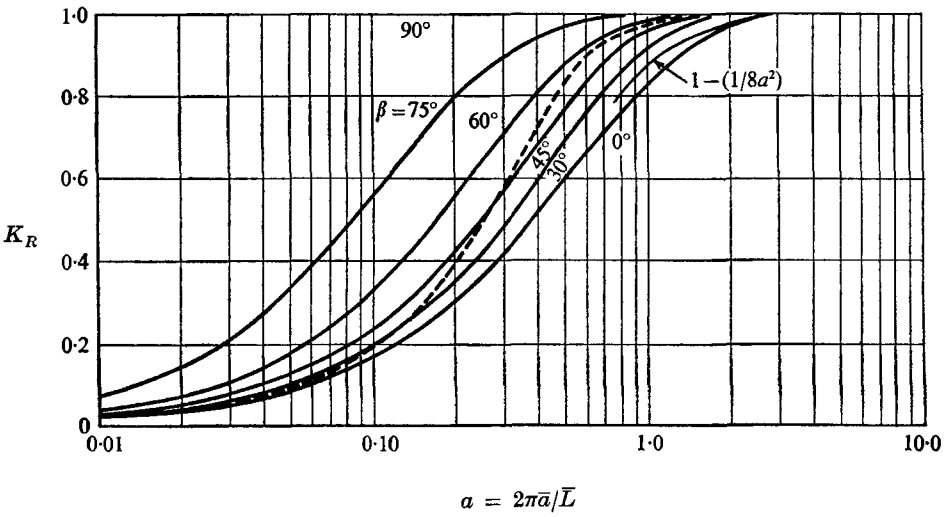

FIGURE 19. Reflexion coefficient. — — , circular cylinder, $\beta = 0°$, Dean & Ursell (1959).

Following that procedure the reflexion coefficient, which is defined as the ratio of the height of the reflected wave to the incident wave, is given by

$$K_R = \left| \frac{ia}{\sqrt{(1-\nu^2/a^2)}} \int_{-1}^{+1} f_4(\xi)\, e^{i\xi a\sqrt{(1-\nu^2/a^2)}}\, d\xi \right|. \tag{55}$$

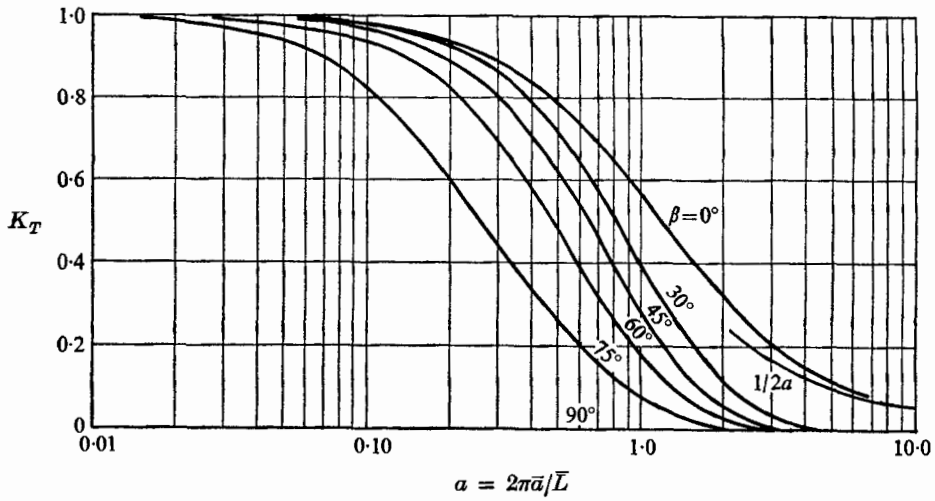

FIGURE 20. Transmission coefficient.

Likewise, the transmission coefficient, which is defined as the ratio of the transmitted to incident wave height, is obtained by using the asymptotic form of Φ' at $x \to +\infty$ and is given by

$$K_T = \left| 1 - \frac{ia}{\sqrt{(1-\nu^2/a^2)}} \int_{-1}^{+1} f_4(\xi)\, e^{-i\xi a\sqrt{(1-\nu^2/a^2)}}\, d\xi \right|. \tag{56}$$

The reflexion and transmission coefficients as obtained from (55) and (56) are plotted in figures 19 and 20, respectively.

Results and discussion

In this paper, the potential problem was solved for an infinite length, zero-draft cylinder oscillating in heave and roll with amplitude varying periodically along its axis as well as the complementary problem associated with the interaction of a fixed zero-draft cylinder with a wave train incident at some oblique angle. The results of the problem are necessarily dependent on the two parameters $a = \sigma^2\bar{a}/g = 2\pi\bar{a}/\bar{L}$ and $\nu = a\sin\beta = (2\pi\bar{a}\sin\beta)/\bar{L} = 2\pi\bar{a}/\bar{l}$. For the case of the cylinder oscillating in still water the forms $a = \sigma^2\bar{a}/g$ and $\nu = 2\pi\bar{a}/\bar{l}$ are the most appropriate form of the parameters. However, for the case of wave interaction with the fixed cylinder, $a = 2\pi\bar{a}/\bar{L}$ and β are the most appropriate forms of the two parameters and the numerical results are presented accordingly.

The results presented in the figures were obtained by use of the numerical procedure discussed but there are certain limiting cases which can be solved directly and used as a check on the numerical results. For the two-dimensional

problem Kim (1965) has obtained the limiting form of the solution for $a \to 0$ as

$$V_i(0) = \lim_{a\to 0} V_i(x,y) = \begin{cases} (1/\pi)\int_{-1}^{+1} f_i^0(\xi)\ln\sqrt{((x-\xi)^2+y^2)}\,d\xi + i0 \\ \text{if } f_i^0(\xi) \text{ is an odd function of } \xi, \\ O(\ln a) - i\int_{-1}^{+1} f_i^0(\xi)\,d\xi \\ \text{if } f_i^0(\xi) \text{ is an even function of } \xi, \end{cases}$$

where $$\tfrac{1}{2}f_i^0(x) + \lim_{y\to 0}(1/\pi)\int_{-1}^{+1} f_i^0(\xi)\frac{\partial}{\partial y}(\ln\sqrt{[(x-\xi)^2+y^2]})\,d\xi = h_i(x).$$

This problem can be solved directly without recourse to approximate methods. The results are

$$f_i^0 = h_i$$

and, accordingly, $$V_3 = \frac{1}{2\pi}\left[2x + (x+1)(x-1)\ln\left(\frac{1-x}{1+x}\right)\right],$$

$$V_2 = V_4 = O(\ln a) = i2.$$

These results provide the following limiting values for the added mass, damping and force coefficients:

$$M_{22} = O(\ln a), \quad N_{22} = 4{\cdot}0, \quad C_2 = 2,$$
$$M_{33} = 1/\pi, \quad N_{33} = 0, \quad C_3 = 0,$$

and the limiting form of the pressure amplitude distribution in roll as

$$\left|\frac{(\bar{\pi}_3)_{\max}}{\rho g \bar{a} x_3^0}\right| = \frac{a}{2\pi}\left[2x + (x+1)(x-1)\ln\left(\frac{1-x}{1+x}\right)\right]. \tag{57}$$

Another check on the accuracy of the numerical results can be made by extending Haskind's relations as advocated by Newman (1962) to the present case. For oblique waves this extension yields the relationship,

$$C_i = \frac{1}{a}\left|\frac{\bar{\eta}_{\max}}{\bar{x}_i^0}\right|\sqrt{(1-\nu^2/a^2)},$$

between the wave force (or moment) coefficient and wave height ratio and, the relationship,

$$N_{ii} = \frac{1}{a^2}\left|\frac{\bar{\eta}_{\max}}{\bar{x}_i^0}\right|^2\sqrt{(1-\nu^2/a^2)},$$

between the damping coefficient and wave height ratio. Accordingly, a correspondence among the heave results presented in figures 11, 15 and 17 as well as among the roll results presented in figures 12, 16 and 18 should be observed. A numerical check on these results shows, in fact, complete agreement.

High-frequency ($a \to \infty$) asymptotic expressions for most of the results presented herein were obtained for the case of $\nu = 0$ by Holford (1964) and can also be used to check the numerical results. These are given as

$$M_{22} = \frac{\pi}{2}\left[1 - \frac{2}{\pi}\frac{\ln a}{a} + O(a)\right], \quad M_{33} = \frac{\pi}{16}\left[1 - \frac{4}{\pi}\frac{\ln a}{a} + O\left(\frac{1}{a}\right)\right],$$

$$N_{22} = \frac{\pi}{2}\left[\frac{2}{a} + O\left(\frac{1}{a^{\frac{3}{2}}}\right)\right], \quad N_{33} = \frac{\pi}{16}\left[\frac{4}{a} + O\left(\frac{1}{a^{\frac{3}{2}}}\right)\right],$$

$$\left|\frac{\overline{\eta}_{\max}}{x_2^0\bar{a}}\right| = (\pi a)^{\frac{1}{2}} + O(1), \quad \left|\frac{\overline{\eta}_{\max}}{x_3^0\bar{a}}\right| = \tfrac{1}{2}(\pi a)^{\frac{1}{2}} + O(1),$$

$$K_R \sim 1 - \frac{1}{8a^2}, \quad K_T \sim \frac{1}{2a}.$$

Using Haskind's relations the asymptotic forms for the force coefficients become

$$C_2 \sim \left(\frac{\pi}{a}\right)^{\frac{1}{2}}, \quad C_3 \sim \frac{1}{2}\left(\frac{\pi}{a}\right)^{\frac{1}{2}}.$$

These asymptotic expressions are shown on the appropriate figures for comparison with the present results.

The limiting case of $\nu \to a$, which corresponds to $\beta \to 90°$, can also be used to check the numerical results. For this case the integral equation approaches the form

$$f_i(x) + a\int_{-1}^{+1} f_i(\xi)\, G(x-\xi, 0)\, d\xi = \begin{cases} 1, & i = 2, \text{ heave}, \\ x, & i = 3, \text{ roll}, \\ 1, & i = 4, \text{ scattering}, \end{cases}$$

where the kernel approaches the form

$$G(x-\xi, 0) \sim \frac{1}{\pi}\int_a^\infty \frac{\sqrt{(\eta^2 - a^2)}\, e^{-|x-\xi|\eta}}{\eta^2}\, d\eta + \frac{i}{\sqrt{(1-\nu^2/a^2)}}.$$

For the case of $i = 2$ and 4 the right side of the integral equation is unity and the solution has the asymptotic form

$$f_2 \sim f_4 \sim \frac{-i\sqrt{(1-\nu^2/a^2)}}{2a} \to 0.$$

However, for the case of roll ($i = 3$) the situation is not as simple. Here $f_3(x)$ is an odd function and, consequently, the integral of its product with the imaginary term in the kernel vanishes leaving

$$f_3(x) + a\int_{-1}^{+1} f_3(x)\, \mathrm{Re}\,[G(x-\xi, 0)]\, d\xi = x,$$

where

$$\mathrm{Re}\,[G(x-\xi, 0)] = \frac{1}{\pi}\int_a^\infty \frac{\sqrt{(\eta^2 - a^2)}\, e^{-|x-\xi|\eta}}{\eta^2}\, d\eta.$$

The solution to this integral equation is not straightforward and, therefore, no elementary function exists for $f_3(x)$. However, the asymptotic form for f_2 and f_4 given above provides the following limiting relationships for $\nu \to a$:

$$\left|\frac{(\overline{\pi}_2)_{\max}}{\rho g x_2^0 \bar{a}}\right| \sim 1, \quad \left|\frac{(\overline{\pi}')_{\max}}{\rho g \bar{a} \eta_w^0}\right| \sim 0,$$

$$C_2 \sim 0, \quad C_3 \sim 0,$$

$$M_{22} \sim 2/a, \quad N_{22} \sim 0,$$

$$K_T \sim 0, \quad K_R \sim 1,$$

$$\left|\frac{\overline{\eta}_{\max}}{x_2^0\bar{a}}\right| \sim 1.$$

The dimensionless pressure amplitude distributions for heaving and rolling motion are shown in figures 6–8 for various values of the parameters ν and a. These results indicate a general increase in pressure amplitude with a and a decrease with ν. For the two-dimensional problem the limiting pressures vanish for $a \to 0$ while for $\nu \neq 0$ the limiting pressure amplitudes clearly approach a non-zero distribution for $a \to \nu$. For heaving motion this limiting distribution is unity. For the two-dimensional case we note that (57) agrees very well with the numerical results of figure 6 for values of a as large as unity.

On figure 6, MacCamy's (1964) results corresponding to $\nu = 0$ are shown for comparison.

Figures 9 and 10 show the pressure amplitude due to wave interaction with a fixed zero-draft cylinder as a function of position on the cylinder and the parameter, $a = 2\pi\bar{a}/\bar{L}$, for various values of the incidence angle, β. Generally it is evident that the pressure amplitudes decrease with increasing the angle of incidence, vanishing at $\beta = 90°$, while the results for $\beta = 0$, corresponding to the two-dimensional case, give the greatest pressure amplitudes.

The variation of the pressure amplitude with position on the cylinder for a given value of a is also interesting. $x = -1$, corresponding to the edge upon which the waves are incident, shows the maximum pressure amplitude with a general decrease across the cylinder. For the long waves, i.e. small values of a, the pressure is essentially constant across the cylinder whereas, for short waves the pressure amplitude rapidly decreases with distance from the leading edge. This illustrates the well-known behaviour that the short waves cannot penetrate under the cylinder while the long waves pass unchanged.

The vertical, or heaving, wave force coefficient is shown in figure 11 as a function of $a = 2\pi\bar{a}/\bar{L}$ and the wave incidence angle, β, along with the asymptotic form for $a \to 0$ and ∞. It is interesting and significant from a practical view point that the two-dimensional case, corresponding to $\beta = 0$, yields the maximum wave force; the effect of incidence is to decrease the force. Although this conclusion has been demonstrated for the zero-draft case only, it can, no doubt, be applied in general and is, therefore, a very important result.

The wave moment coefficient is shown in figure 12 as a function of $a = 2\pi\bar{a}/\bar{L}$ for various values of β along with the two-dimensional asymptotic forms for $a \to 0$ and ∞. It is interesting that for the two-dimensional case the maximum value of the moment coefficient occurs at approximately $a = 1{\cdot}5$ or $2\bar{a} = \frac{1}{2}\bar{L}$. This is in agreement with intuition since the maximum differences in pressure in the incident wave occurs between the crest and trough, i.e. within half a wavelength, and one would expect this to produce the maximum moment.

The added mass and moment of inertia coefficients are presented in figures 13 and 14. The two-dimensional added mass coefficient in heave is logarithmically singular at $a = 0$ while the added moment of inertia coefficient has a limiting value of $1/\pi$. The asymptotic expressions for $a \to \infty$ for both M_{22} and M_{33} are also shown on the figures for comparison.

We note that MacCamy (1964) also has presented numerical values for M_{22} and M_{33} for $\nu = 0$ which are in agreement with the present results although they are not presented.

The damping coefficients in heave and roll are shown in figures 15 and 16, respectively. In either case the effect of ν is similiar; increasing ν tends to decrease the damping. In these figures the damping is seen to vanish when $a = \nu$ in agreement with the limiting form of the solution. This feature may be interpreted physically as being due to the condition that when $a = \nu$ ($\beta = 90°$) the wave crests are perpendicular to the axis of the cylinder and, therefore, no energy is propagated away from the cylinder in the $\pm x$ directions. Consequently, the damping coefficient, which is associated with this energy flux, must be zero.

MacCamy (1964) has also presented numerical results for N_{22} and N_{33} for the two-dimensional case which are in agreement with the present results.

The low-frequency approximation for the damping coefficient in roll for the two-dimensional case may be obtained as a special case of that for an elliptical cylinder as determined by Kotik & Mangulis (1962) as

$$N_{33} = \tfrac{4}{9}a^2 + O(a^2).$$

For comparison we plot $\frac{4}{9}a^2$ in figure 16. We also find the present numerical results in agreement with the limiting value of $N_{22} = 4{\cdot}0$ at $a = \nu = 0$.

The high-frequency ($a \to \infty$) asymptotic expression for the two-dimensional case as determined by Holford (1964) for N_{22} is shown in figure 15. The corresponding asymptotic expression, $N_{33} = \frac{1}{4}\pi(1/a)$, is still well above the numerical results at the largest value of a on figure 16.

The wave height ratios for heave and roll are shown in figures 17 and 18 and, generally, both of these curves indicate the same effect of $\nu = 2\pi\bar{a}/\bar{l}$; increasing ν decreases the wave height ratios.

On figure 17 Holford's two-dimensional high-frequency ($a \to \infty$) asymptotic expression is shown. The corresponding asymptotic expression for roll is still well above the $\nu = 0$ curve indicated in figure 18.

Figures 19 and 20 show the reflexion and transmission coefficients, respectively, as a function of the parameters, $a = 2\pi\bar{a}/\bar{L}$ and β for the fixed, zero-draft cylinder along with the short wave asymptotic expressions. As indicated by the figure, increasing β corresponds to increasing reflexion coefficients with a limiting value of unity at $\beta = 90°$. The two-dimensional case shows the greatest transmission and least reflexion and, therefore, is the most critical case in the design of breakwaters. This is a very important result to those involved in testing since most test work is carried out in two-dimensional wave tanks.

We note that Levine's (1965) results for a completely submerged circular cylinder show the same general trends with no reflexion occurring at $\beta = 0$ and complete reflexion occurring at $\beta = 90°$.

The curve attributed to Dean & Ursell (1959) for a semi-submerged circular cylinder was included for comparison to illustrate the effect of draft.

Appendix A

The infinite integral term in the Green's function given in (30) was arranged in a number of parts, one of which was analytically integrable and two of which required numerical integration. As part of the numerical evaluation of the

second of these integrals, as it appears in (33), it was necessary to replace the infinite upper limit with some suitable large number. The question arises as to the magnitude of the error introduced by this approximation. To put bounds on the maximum possible error we compare the portion of the integral neglected to the total infinite integral term as given in (30). Replacing ν in the lower limit of the original integral term by P, where $P \gg \nu$, we have for the error, e,

$$e < \frac{\int_P^\infty \frac{(\eta - \sqrt{(\eta^2-\nu^2)})}{(\eta^2+a^2-\nu^2)} e^{-|x-\xi|\eta}\, d\eta}{\int_P^\infty \frac{\sqrt{(\eta^2-\nu^2)}}{(\eta^2+a^2-\nu^2)} e^{-|x-\xi|\eta}\, d\eta}.$$

Both the maximum value of $(\eta - \sqrt{(\eta^2-\nu^2)})$ and the minimum value of $\sqrt{(\eta^2-\nu^2)}$ occur at $\eta = P$. Thus,

$$e < \frac{P/\nu - \sqrt{(P^2/\nu^2-1)}}{\sqrt{(P^2/\nu^2-1)}}.$$

Using $P/\nu = 50$ we find $$e < \frac{1}{5000}.$$

Appendix B

The purpose of this appendix is to show that the approximate relationship, (37) converges to (36) for the logarithmic term occurring in G when $i = j+1$. That is, carrying out the integration of the logarithmic term analytically over the $i = j+1$ interval according to (36) gives

$$\int_{x_{j+1}-\Delta x/2}^{x_{j+1}+\Delta x/2} \ln|x_j - t|\, dt = \Delta x \ln \Delta x - 0{\cdot}044\, \Delta x, \tag{B 1}$$

and by use of (37) we obtain

$$\Delta x \ln|x_j - x_{j+1}| = \Delta x \ln \Delta x. \tag{B 2}$$

Thus, comparing expressions (B 1) and (B 2) it is evident that the result given by (37) does, in fact, converge to that given by (36) for $2/m = \Delta x \to 0$.

For $m = 40$ we find the ratio of (B 2) to (B 1) to be

$$\left.\frac{\ln \Delta x}{\ln(\Delta x) - 0{\cdot}044}\right|_{\Delta x = 1/20} = 0{\cdot}985. \tag{B 3}$$

Thus, an error of 1·5 % is introduced by using (37) instead of (36) for the most critical element of $i = j+1$.

REFERENCES

DEAN, R. G. & URSELL, F. 1959 Interaction of a fixed, semi-immersed circular cylinder with a train of surface waves. *Tech. Rep.* no. 37, *Hydro. Lab.*, M.I.T.

GIDLUND, E. R. 1963 Interaction effects between surface waves and fixed semi-immersed obstacles by potential theory. Ph.D. dissertation, University of Washington (unpublished).

GRÖBNER, W. & HOFREITER, N. 1966 *Intergraltafeln.* New York: Springer.

HOLFORD, R. L. 1964 Short surface waves in the presence of a finite dock. II. *Proc. Cam. Phil. Soc.* **60**, 985–1011.

JOHN, F. 1950 On the motion of floating bodies. II. *Comm. Pure Appl. Math.* **3**, 45–101.

KIM, W. D. 1965 On the harmonic oscillations of a rigid body on a free surface. *J. Fluid Mech.* **21**, 427–451.

KOTIK, J. & MANGULIS, V. 1962 Some low-frequency damping coefficients for sections and bodies. *Tech. Rep., Res. Group, Contract Nonr*-2692(00), *Office of Naval Research.*

LEVINE, H. 1965 Scattering of surface waves by a submerged circular cylinder. *J. Math. Phys.* **6**, 1231–1243.

MACCAMY, R. C. 1957 A source solution for short crested waves. *La Houille Blanche*, **3**, 379–389.

MACCAMY, R. C. 1961 On the heaving motion of cylinders of shallow draft. *J. Ship Res.* **5**, no. 3, 34–43.

MACCAMY, R. C. 1964 The motion of cylinders of shallow draft. *J. Ship Res.* **7**, no. 3, 1–11.

NEWMAN, J. N. 1962 The exciting forces on fixed bodies in waves. *J. Ship Res.* **6**, 10–17.

PORTER, W. R. 1960 Pressure distribution, added-mass and damping coefficients for cylinders oscillating in a free surface. *Tech. Rep., series* 82, *issue* 16, *Inst. Engr. Res., University of California, Berkeley.*

URSELL, F. 1949 On the heaving motion of a circular cylinder on the surface of a fluid. *Quart. J. Mech. Appl. Math.* **2**, 218–231.

YU, Y. S. & URSELL, F. 1961 Surface waves generated by an oscillating circular cylinder on water of finite depth: theory and experiment. *J. Fluid Mech.* **11**, 529–551.